



UNIVERSITY OF LEEDS

This is a repository copy of *Insight into structure: function relationships in a molecular spin-crossover crystal, from a related weakly cooperative compound*.

White Rose Research Online URL for this paper:  
<http://eprints.whiterose.ac.uk/83008/>

Version: Accepted Version

---

**Article:**

Elhaïk, J, Kilner, C and Halcrow, MA (2014) Insight into structure: function relationships in a molecular spin-crossover crystal, from a related weakly cooperative compound. *European Journal of Inorganic Chemistry*, 2014 (26). 4250 - 4253. ISSN 1434-1948

<https://doi.org/10.1002/ejic.201402623>

---

**Reuse**

Items deposited in White Rose Research Online are protected by copyright, with all rights reserved unless indicated otherwise. They may be downloaded and/or printed for private study, or other acts as permitted by national copyright laws. The publisher or other rights holders may allow further reproduction and re-use of the full text version. This is indicated by the licence information on the White Rose Research Online record for the item.

**Takedown**

If you consider content in White Rose Research Online to be in breach of UK law, please notify us by emailing [eprints@whiterose.ac.uk](mailto:eprints@whiterose.ac.uk) including the URL of the record and the reason for the withdrawal request.

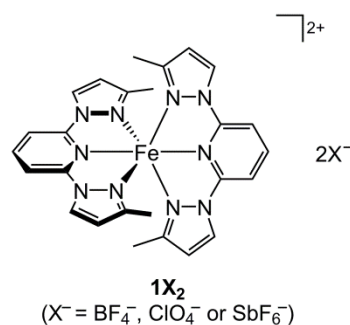


[eprints@whiterose.ac.uk](mailto:eprints@whiterose.ac.uk)  
<https://eprints.whiterose.ac.uk/>

# Insight into Structure:Function Relationships in a Molecular Spin-Crossover Crystal, from a Related Weakly Cooperative Compound

Jérôme Elhaïk,<sup>[a]</sup> Colin A. Kilner,<sup>[a]</sup> and Malcolm A. Halcrow<sup>\*[a]</sup>

**Abstract:** The  $\text{ClO}_4^-$  salt of  $[\text{FeL}_2]^{2+}$  ( $L = 2,6\text{-bis}(3\text{-methylpyrazol-1-yl})\text{pyridine}$ ) undergoes very gradual thermal spin-crossover centered just below room temperature. In contrast, the  $\text{BF}_4^-$  salt of the same complex exhibits an abrupt and structured spin-transition at lower temperature, with a complicated structural chemistry. The difference can be attributed to a much larger change in molecular structure between the spin states of the complex in the more cooperative  $\text{BF}_4^-$  salt, leading to an increased kinetic barrier for their interconversion. Consistent with that suggestion, the high-spin and low-spin structures of weakly cooperative  $[\text{FeL}_2][\text{ClO}_4]_2$  are almost superimposable.



**Scheme 1.** The compounds discussed in this work.

The continuing interest in thermally and optically switchable spin-crossover (SCO) materials<sup>[1-3]</sup> reflects their potential use in display and memory devices,<sup>[4]</sup> as reporter groups in sensors<sup>[5]</sup> and imaging applications,<sup>[6]</sup> and in nanoscience.<sup>[7]</sup> Many of these applications require materials exhibiting cooperative spin-state switching; that is, abruptly and with thermal hysteresis. Understanding the structural factors underlying the cooperativity of SCO, and the design of new materials with useful switching properties, are important challenges for crystal engineering.<sup>[8]</sup>

Some years ago we reported  $[\text{FeL}_2][\text{BF}_4]_2 \cdot x\text{H}_2\text{O}$  (**1** $[\text{BF}_4]_2 \cdot x\text{H}_2\text{O}$ ;  $L = 2,6\text{-bis}(3\text{-methylpyrazol-1-yl})\text{pyridine}$ ;  $x = 0\text{-}\frac{1}{3}$ ; Scheme 1), whose spin-state properties are unusual for several reasons.<sup>[9]</sup> Its thermal spin-transition takes place in two steps, *via* a re-entrant symmetry-breaking transition to an intermediate crystal phase, with a tripled unit cell containing a mixture of high-spin and low-spin sites. The first of these steps occurs abruptly with hysteresis, but at a temperature that varies according to the water content of the sample ( $x$ ). In contrast the second step is kinetically slow, and is only achieved when the sample is poised at 100 K for 1.5 hrs.<sup>[10]</sup> Its excited spin-state trapping (LIESST<sup>[11]</sup>) behavior is also unique, in that its thermodynamic high $\rightarrow$ low spin transition and kinetically controlled high $\rightarrow$ low spin-state relaxation exhibit different profiles and are effectively decoupled from each other.<sup>[9]</sup> In the light of these unusual results we were keen to compare **1** $[\text{BF}_4]_2$  with other salts of the  $[\text{FeL}_2]^{2+}$  dication, and report here the close analogue  $[\text{FeL}_2][\text{ClO}_4]_2$  (**1** $[\text{ClO}_4]_2$ ; Scheme 1). This compound is not isostructural with **1** $[\text{BF}_4]_2$  and shows very different spin-state

characteristics.<sup>[12]</sup> Although unexceptional in itself, **1** $[\text{ClO}_4]_2$  provides useful insight into the structural origin of the unusual behavior of the  $\text{BF}_4^-$  salt by providing a rare comparison between strongly and weakly cooperative spin-crossover materials based on the same complex molecule.<sup>[13]</sup>

Reaction of  $\text{Fe}[\text{ClO}_4]_2 \cdot 6\text{H}_2\text{O}$  with 2 equiv of  $L$ <sup>[14]</sup> in methanol at room temperature affords a mustard yellow solution. Slow diffusion of diethyl ether into the concentrated solution yields red crystals, that were formulated as the expected product  $[\text{FeL}_2][\text{ClO}_4]_2$  (**1** $[\text{ClO}_4]_2$ ) by microanalysis and mass spectrometry. Since iron(II) complexes of 2,6-dipyrazolylpyridine derivatives are usually yellow in their high-spin state and brown in their low-spin form, the red color of **1** $[\text{ClO}_4]_2$  implies that it exists as a mixture of spin-states at room temperature. That was borne out by the measurements described below. Recrystallization of **1** $[\text{ClO}_4]_2$  from acetone, acetonitrile or nitromethane all yielded mixtures of solvent-free and solvated phases of the complex.<sup>[13]</sup> However, material obtained from methanol/diethyl ether was phase-pure, unsolvated **1** $[\text{ClO}_4]_2$  by  $X$ -ray powder diffraction.<sup>[10]</sup> Magnetochemical experiments were performed using polycrystalline samples of the complex prepared in this manner.

At 300 K,  $\chi_M T$  for **1** $[\text{ClO}_4]_2$  is  $2.4 \text{ cm}^3 \text{ mol}^{-1} \text{ K}$ , lower than expected for a high-spin iron(II) complex with this ligand type ( $3.4\text{-}3.6 \text{ cm}^3 \text{ mol}^{-1} \text{ K}$ ).<sup>[15]</sup> As the temperature is lowered,  $\chi_M T$  decreases slowly, becoming effectively zero at around 80 K (Fig. 1). This is consistent with the compound undergoing an extremely gradual thermal spin-transition. The midpoint  $T_{1/2}$  can be estimated at  $267 \pm 2 \text{ K}$ , and 68% of the sample is in its high-spin state at 300 K if  $\chi_M T$  for the high-spin compound is estimated as  $3.5 \text{ cm}^3 \text{ mol}^{-1} \text{ K}$ . The transition is 95 % complete near 150 K, the remaining 5% of the sample converting extremely slowly as the temperature is lowered further. Extrapolation of the susceptibility data implies that the complex only becomes fully high-spin at a temperature near 400 K.

[a] Dr Jérôme Elhaïk, Colin A. Kilner and Prof Malcolm A. Halcrow  
School of Chemistry, University of Leeds,  
Woodhouse Lane,  
Leeds LS2 9JT, UK.  
E-mail: m.a.halcrow@leeds.ac.uk  
<http://www.chem.leeds.ac.uk/People/Halcrow.html>

Supporting information for this article is given via a link at the end of the document.

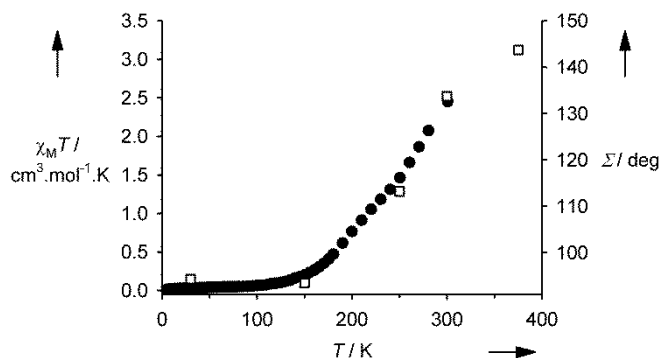


**Figure 1.** Comparison of the SCO transition in **1[ClO<sub>4</sub>]<sub>2</sub>** as measured by magnetic susceptibility data from (●) and X-ray crystallography ( $\Sigma$ , □). See the Supporting Information for the definition of  $\Sigma$ ,<sup>[14]</sup> and a Table containing these values.<sup>[10]</sup>

Single crystal structure determinations of **1[ClO<sub>4</sub>]<sub>2</sub>** were carried out at five different temperatures between 30 and 375 K. The compound retains the same space group (*C2/c*, *Z* = 8) throughout this temperature range, although the quality of the crystals decreased markedly upon cooling. Hence, the precision of the structure at 30 K is somewhat lower than at the higher temperatures, even though those data were collected using a different diffractometer fitted with a more intense X-ray source. While **1[ClO<sub>4</sub>]<sub>2</sub>** crystallizes in the same space group as **1[BF<sub>4</sub>]<sub>2</sub>·xH<sub>2</sub>O** their unit cell dimensions are different and the two compounds are not isostructural. The complex has the expected six-coordinate structure, with only small deviations from the *D<sub>2d</sub>* symmetry expected with this ligand geometry (Fig. 2). The Fe–N bond lengths in **1[ClO<sub>4</sub>]<sub>2</sub>** are equal within experimental error at 30 and 150 K, and very similar to those found in low-spin **1[BF<sub>4</sub>]<sub>2</sub>·xH<sub>2</sub>O**,<sup>[9]</sup> but increase steadily as the temperature is raised further.<sup>[10]</sup> The temperature dependence of  $\Sigma$  and  $\theta$ , which are bond angle parameters that are often used to monitor the spin-states of metal complexes,<sup>[16]</sup> closely mirrors the magnetic susceptibility data (Fig. 1).<sup>[10]</sup> By these measures, **1[ClO<sub>4</sub>]<sub>2</sub>** is low-spin in the crystal at 30 and 150 K, and is predominantly (but not fully) high-spin at 375 K.<sup>[15]</sup>

In contrast to many other complexes from the iron(II)/dipyrazolopyridine family,<sup>[17,18]</sup> the cations in **1[ClO<sub>4</sub>]<sub>2</sub>** do not aggregate through intermolecular  $\pi\cdots\pi$  interactions in the crystal. This presumably reflects the steric bulk of the *L* methyl substituents, preventing close approach of the pyrazole rings on neighboring molecules.<sup>[9,19]</sup> There are two close intermolecular C–H... $\pi$  contacts between cations in the lattice, C(17)–H(17)...C(24) and C(35)–H(35)...C(16<sup>ii</sup>) (symmetry codes (i) *x*, 1–*y*, <sup>1</sup>/<sub>2</sub>+*z*; (ii) <sup>3</sup>/<sub>2</sub>–*x*, <sup>3</sup>/<sub>2</sub>–*y*, 1–*z*), with H...C distances of 2.7±0.1 Å at 300 and 150 K, up to 0.3 Å shorter than the sum of the van der Waals radii of a H atom and an aryl group.<sup>[19]</sup> These are probably responsible for the slightly S-shaped conformations of the coordinated *L* ligands. Otherwise, the complex molecules in the lattice of **1[ClO<sub>4</sub>]<sub>2</sub>** interact through van der Waals contacts only. There are also likely to be weak C–H...O hydrogen bonds between the cations and anions in the lattice, although these cannot be discussed in detail because of the anion disorder. A comparable distribution of intermolecular contacts is also present in crystals of **1[BF<sub>4</sub>]<sub>2</sub>·xH<sub>2</sub>O**.<sup>[9]</sup>

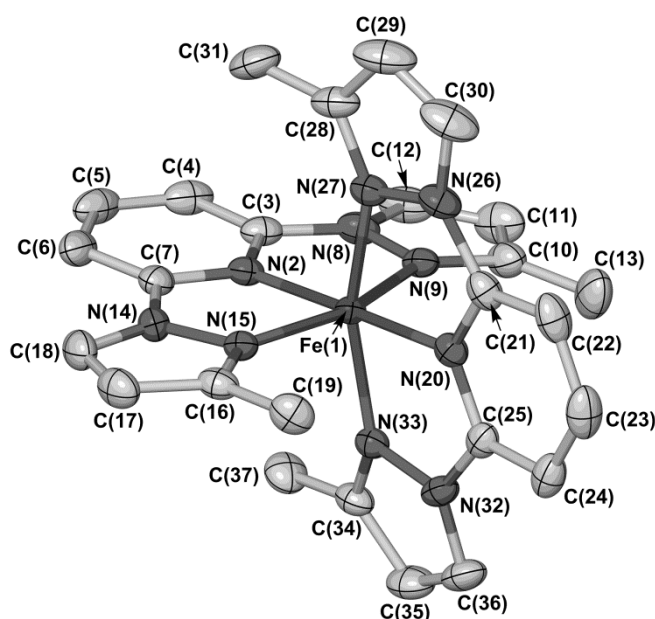


**Figure 2.** View of the complex dication in the crystal structure of **1[ClO<sub>4</sub>]<sub>2</sub>** at 150 K, showing the atom numbering scheme employed. Displacement ellipsoids are at the 50 % probability level, and H atoms have been omitted for clarity.

Despite their chemical similarity, the spin state properties of **1[BF<sub>4</sub>]<sub>2</sub>·xH<sub>2</sub>O** and **1[ClO<sub>4</sub>]<sub>2</sub>** are very different. As described above, **1[BF<sub>4</sub>]<sub>2</sub>·xH<sub>2</sub>O** undergoes a highly cooperative spin-transition below 150 K, that proceeds *via* two crystallographic phase changes, exhibits slow kinetics and is dependent on the presence or absence of lattice water.<sup>[9,10]</sup> In contrast **1[ClO<sub>4</sub>]<sub>2</sub>** exhibits a very gradual SCO equilibrium that is centred just below room temperature, but spans a temperature range of *ca.* 250 K (Fig. 1). The compounds are not isostructural, but there are no aspects of the crystal packing in either compound that could rationalize their different behavior. However, more insight is gained by comparing the molecular structures of the two salts in their high-spin and low-spin states. Apart from the expected differences in Fe–N bond lengths, the high-spin and low-spin structures of the [FeL<sub>2</sub>]<sup>2+</sup> cation in **1[ClO<sub>4</sub>]<sub>2</sub>** are almost superimposable (Fig. 3, top). In contrast, the complex's structure changes much more strongly between the spin states in **1[BF<sub>4</sub>]<sub>2</sub>**, reflecting the relative orientation of the *L* ligands which are canted by *ca.* 15° in the high-spin molecule but are closer to perpendicular in the low-spin state (Fig. 3, bottom). Thus the angle between the least squares planes of the two *L* ligands ( $\theta$ ) in **1[BF<sub>4</sub>]<sub>2</sub>** increases from 76.4 to 81.9° during the transition; that is,  $\Delta\theta = 5.5^\circ$ . In contrast  $\Delta\theta = 0.21(5)^\circ$  for **1[ClO<sub>4</sub>]<sub>2</sub>**, showing that the shape of the complex does not change significantly during SCO in that salt. The molecular structure of **1[ClO<sub>4</sub>]<sub>2</sub>** in both spin-states resembles the low-spin state of **1[BF<sub>4</sub>]<sub>2</sub>**.<sup>[10]</sup> Hence the structural rearrangement during the spin-transition in **1[BF<sub>4</sub>]<sub>2</sub>·xH<sub>2</sub>O** (Fig. 3) reflects crystallographically imposed structural distortions in its high-spin [FeL<sub>2</sub>]<sup>2+</sup> cation.

We have proposed that the occurrence of cooperative spin-transitions in several molecular compounds, including **1[BF<sub>4</sub>]<sub>2</sub>·xH<sub>2</sub>O**, is related to the change in shape of the complex

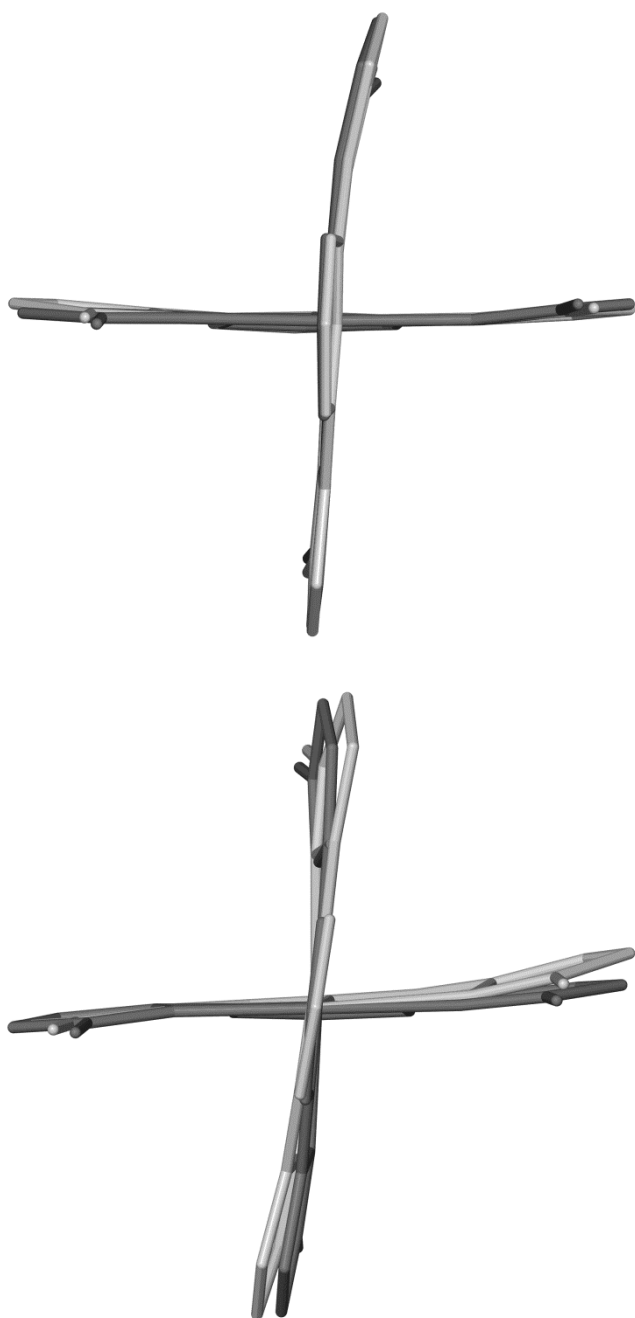


**Figure 3.** Top: overlay of the structures of **1[ClO<sub>4</sub>]<sub>2</sub>** at 375 K (pale) and at 150 K (dark). Bottom: equivalent overlay of the high-spin (pale) and low-spin (dark) structures of **1[BF<sub>4</sub>]<sub>2</sub>**,<sup>[9]</sup> emphasizing the greater structural changes occurring during SCO for the BF<sub>4</sub><sup>-</sup> salt.

between the spin states.<sup>[8]</sup> Spin-transitions inducing a conformational change at the ligand periphery will require a much greater rearrangement of the crystalline structure, than other examples involving a simple breathing of the lattice. Hence spin transitions involving a change in molecular shape should have a higher activation barrier and higher cooperativity, all other things being equal. This study bears out those ideas, since **1[ClO<sub>4</sub>]<sub>2</sub>** exhibits much smaller structural differences between its

high and low-spin states than the BF<sub>4</sub><sup>-</sup> salt, and correspondingly undergoes a more gradual thermal spin-equilibrium. Our current work aims to apply these results to the bottom-up design of new SCO materials with technologically favorable switching properties, based on efficient mechanical coupling between switching centres.<sup>[18,21]</sup>

## Experimental Section

**Instrumentation:** Electrospray mass spectra were obtained using a Waters Micromass LCT TOF spectrometer, in a MeOH matrix. CHN microanalyses were performed by the University of Leeds Department of Chemistry microanalytical service. Magnetic susceptibility measurements were obtained using a Quantum Design SQUID magnetometer in an applied field of 1000 G. Diamagnetic corrections were estimated from Pascal's constants.<sup>[22]</sup> X-ray powder diffraction measurements were obtained from a Bruker D2 Phaser diffractometer, using Cu K<sub>α</sub> radiation ( $\lambda = 1.5419 \text{ \AA}$ ).

**Synthesis of 1[ClO<sub>4</sub>]<sub>2</sub>.** A mixture of Fe[ClO<sub>4</sub>]<sub>2</sub>·6H<sub>2</sub>O (0.16 g, 0.43 mmol) and L<sup>[14]</sup> (0.21 g, 0.87 mmol) in methanol (40 cm<sup>3</sup>) was stirred at room temperature until all the solid had dissolved. The yellow solution was concentrated to ca 5 cm<sup>3</sup> under reduced pressure and filtered. Slow diffusion of diethyl ether into the solution yielded homogeneous red crystals of the product. Yield 0.20 g, 64 %. Found C, 42.5; H, 3.40; N, 19.3 %. Calcd. for C<sub>26</sub>H<sub>26</sub>Cl<sub>2</sub>FeN<sub>10</sub>O<sub>8</sub> C, 42.6; H, 3.57; N, 19.1 %. ES mass spectrum (MeCN) *m/z* 267 [<sup>56</sup>FeL<sub>2</sub>]<sup>2+</sup>, 240 [L+H]<sup>+</sup>. **CAUTION** Although we have experienced no problems in handling this compound, metal-organic perchlorates are potentially explosive and should be handled with due care in small quantities.

**Crystal data for 1[ClO<sub>4</sub>]<sub>2</sub>.** C<sub>26</sub>H<sub>26</sub>Cl<sub>2</sub>FeN<sub>10</sub>O<sub>8</sub>, *M<sub>r</sub>* = 733.32 gmol<sup>-1</sup>, monoclinic, *C*2/*c*, *Z* = 8, *F*(000) = 3008. At *T* = 375 K: *a* = 35.7428(3) Å, *b* = 11.4376(1) Å, *c* = 17.3740(2) Å,  $\beta$  = 114.5348(7) °, *V* = 6461.39(11) Å<sup>3</sup>,  $\rho_{\text{calcd.}}$  = 1.508 g cm<sup>-3</sup>,  $\mu$  (Mo-K $\alpha$ ) = 0.695 cm<sup>-1</sup>, 62437 reflections in *h*(-46/46), *k*(-14/14), *l*(-22/22), measured in the range 1.89° ≤  $\theta$  ≤ 27.52°, completeness  $\theta_{\text{max}}$  = 98.8 %, 7355 independent reflections, *R*<sub>int</sub> = 0.092, 5568 reflections with *F*<sub>0</sub> > 4 $\sigma$ (*F*<sub>0</sub>), 440 parameters, 50 restraints, *R*<sub>1obs</sub> = 0.067, *wR*<sub>2obs</sub> = 0.202, *R*<sub>1all</sub> = 0.083, *wR*<sub>2all</sub> = 0.227, GooF = 1.052, largest difference peak and hole: 0.43/-0.43 eÅ<sup>-3</sup>. At *T* = 300 K: *a* = 35.3582(3) Å, *b* = 11.3693(2) Å, *c* = 17.2346(2) Å,  $\beta$  = 114.3000(7) °, *V* = 6314.45(14) Å<sup>3</sup>,  $\rho_{\text{calcd.}}$  = 1.543 g cm<sup>-3</sup>,  $\mu$  (Mo-K $\alpha$ ) = 0.712 cm<sup>-1</sup>, 60351 reflections in *h*(-45/45), *k*(-14/14), *l*(-22/22), measured in the range 1.26° ≤  $\theta$  ≤ 27.48°, completeness  $\theta_{\text{max}}$  = 99.6 %, 7212 independent reflections, *R*<sub>int</sub> = 0.082, 5549 reflections with *F*<sub>0</sub> > 4 $\sigma$ (*F*<sub>0</sub>), 440 parameters, 50 restraints, *R*<sub>1obs</sub> = 0.062, *wR*<sub>2obs</sub> = 0.173, *R*<sub>1all</sub> = 0.079, *wR*<sub>2all</sub> = 0.194, GooF = 1.052, largest difference peak and hole: 0.51/-0.54 eÅ<sup>-3</sup>. At *T* = 250 K: *a* = 34.9296(5) Å, *b* = 11.2753(2) Å, *c* = 17.1040(3) Å,  $\beta$  = 114.1340(11) °, *V* = 6147.46(18) Å<sup>3</sup>,  $\rho_{\text{calcd.}}$  = 1.585 g cm<sup>-3</sup>,  $\mu$  (Mo-K $\alpha$ ) = 0.731 cm<sup>-1</sup>, 59707 reflections in *h*(-44/44), *k*(-14/14), *l*(-21/22), measured in the range 2.39° ≤  $\theta$  ≤ 27.57°, completeness  $\theta_{\text{max}}$  = 98.1 %, 6978 independent reflections, *R*<sub>int</sub> = 0.118, 5568 reflections with *F*<sub>0</sub> > 4 $\sigma$ (*F*<sub>0</sub>), 440 parameters, 50 restraints, *R*<sub>1obs</sub> = 0.068, *wR*<sub>2obs</sub> = 0.177, *R*<sub>1all</sub> = 0.085, *wR*<sub>2all</sub> = 0.191, GooF = 1.150, largest difference peak and hole: 0.70/-0.60 eÅ<sup>-3</sup>. At *T* = 150 K: *a* = 34.4667(3) Å, *b* = 11.1688(1) Å, *c* = 17.0142(2) Å,  $\beta$  = 113.8974(5) °, *V* = 5988.18(10) Å<sup>3</sup>,  $\rho_{\text{calcd.}}$  = 1.627 g cm<sup>-3</sup>,  $\mu$  (Mo-K $\alpha$ ) = 0.750 cm<sup>-1</sup>, 49516 reflections in *h*(-44/41), *k*(-14/14), *l*(-22/22), measured in the range 1.29° ≤  $\theta$  ≤ 27.62°, completeness  $\theta_{\text{max}}$  = 98.7 %, 6898 independent reflections, *R*<sub>int</sub> = 0.095, 6351 reflections with *F*<sub>0</sub> > 4 $\sigma$ (*F*<sub>0</sub>), 440 parameters, 50 restraints, *R*<sub>1obs</sub> = 0.061, *wR*<sub>2obs</sub> = 0.141, *R*<sub>1all</sub> = 0.066, *wR*<sub>2all</sub> = 0.144, GooF = 1.167, largest difference peak and hole: 0.87/-0.65 eÅ<sup>-3</sup>. At *T* = 30 K: *a* = 34.353(3) Å, *b* = 11.1539(8) Å, *c* = 17.0594(12) Å,  $\beta$  = 113.812(4) °, *V* = 5980.2(7) Å<sup>3</sup>,

$\rho_{\text{calcd.}} = 1.629 \text{ g cm}^{-3}$ ,  $\mu$  (Mo-K $\alpha$ ) =  $0.751 \text{ cm}^{-1}$ , 26660 reflections in  $h(-41/43)$ ,  $k(-12/14)$ ,  $l(-21/21)$ , measured in the range  $1.30^\circ \leq \theta \leq 2705^\circ$ , completeness  $\theta_{\text{max}} = 97.4\%$ , 6376 independent reflections,  $R_{\text{int}} = 0.072$ , 4824 reflections with  $F_0 > 4\sigma(F_0)$ , 474 parameters, 20 restraints,  $R_{\text{1obs}} = 0.080$ ,  $wR_{\text{2obs}} = 0.186$ ,  $R_{\text{1all}} = 0.107$ ,  $wR_{\text{2all}} = 0.196$ , GooF = 1.294, largest difference peak and hole:  $0.61/-0.79 \text{ e}\text{\AA}^{-3}$ .

Diffraction data were collected with a Bruker X8 Apex II diffractometer diffractometer, using graphite-monochromated Mo-K $\alpha$  radiation ( $\lambda = 0.71073 \text{ \AA}$ ) generated by a rotating anode. The structure was solved by direct methods (SHELXS-97),<sup>[23]</sup> then developed by least squares refinement on  $F^2$  (SHELXL-97).<sup>[23]</sup> Crystallographic figures were prepared using XSEED.<sup>[24]</sup> At 30 K, one of the two  $\text{ClO}_4^-$  anions was disordered over two orientations, labelled 'A' and 'B'. The occupancies of these two sites refined to 0.49 and 0.51, respectively, so they were each refined with half-occupancy in the final analysis. The Cl–O bonds in this anion were restrained to  $1.44(2) \text{ \AA}$ , and O...O distances within each partial anion environment to  $2.35(2) \text{ \AA}$ . All non-H atoms in this structure were refined anisotropically, while all H atoms were placed in calculated positions and refined using a riding model. At 150 K and above, both  $\text{ClO}_4^-$  anions were disordered. One of these was modelled over two equally occupied sites, while the other was modelled over three orientations with occupancies of 0.4, 0.3 and 0.3. Similar restraints were applied to these disordered anions, at each temperature, as described above for the 30 K structure. At these temperatures only the wholly occupied non-H atoms were refined anisotropically, while H atoms were placed in calculated positions and refined using a riding model.

CCDC-1007267–1007271 contains the supplementary crystallographic data for this paper. These data can be obtained free of charge from the Cambridge Crystallographic Data Centre via [www.ccdc.cam.ac.uk/data\\_request/cif](http://www.ccdc.cam.ac.uk/data_request/cif).

## Acknowledgements

The authors thank Dr. V. A. Money and Professor J. A. K. Howard (University of Durham, UK) for help with the crystallographic studies, and Dr H. J. Blythe (University of Sheffield, UK) for the susceptibility data. This work was funded by the EPSRC.

**Keywords:** iron • N ligands • spin-crossover • X-ray crystallography

- [1] P. Gütlich, H. A. Goodwin (Eds.), *Spin-Crossover in Transition-Metal Compounds I–III*, in: *Topics in Current Chemistry*, vol. 233–235, Springer, Berlin, 2004.
- [2] M. A. Halcrow (Ed.), *Spin-crossover materials - properties and applications*, John Wiley & Sons, Chichester, UK, 2013, p. 568.
- [3] P. Gütlich, *Eur. J. Inorg. Chem.* **2013**, 581–591.
- [4] O. Kahn, C. J. Martinez, *Science* **1998**, *279*, 44–48.
- [5] J. Linares, E. Codjovi, Y. Garcia, *Sensors* **2012**, *12*, 4479–4492; O. S. Wenger, *Chem. Rev.* **2013**, *113*, 3686–3733.
- [6] J. Hasserodt, J. Kolanowski, F. Touti, *Angew. Chem.* **2014**, *126*, 60–75; *Angew. Chem. Int. Ed.* **2014**, *53*, 60–73; I.-R. Jeon, J. G. Park, C. R. Haney, T. D. Harris, *Chem. Sci.* **2014**, *5*, 2461–2465.
- [7] M. Cavallini, *Phys. Chem. Chem. Phys.* **2012**, *14*, 11867–11876; H. J. Shepherd, G. Molnár, W. Nicolazzi, L. Salmon, A. Bousseksou, *Eur. J. Inorg. Chem.* **2013**, 653–661.
- [8] M. A. Halcrow, *Chem. Soc. Rev.* **2011**, *40*, 4119–4142.
- [9] V. A. Money, C. Carbonera, J. Elhaik, M. A. Halcrow, J. A. K. Howard, J.-F. Létard, *Chem. Eur. J.* **2007**, *13*, 5503–5514.

- [10] Additional crystallographic Figures, Tables of bond lengths and angles, X-ray powder diffraction data and a comparison of the spin-crossover behaviour of **1**[ $\text{ClO}_4$ ]<sub>2</sub> and **1**[ $\text{BF}_4$ ]<sub>2</sub>·xH<sub>2</sub>O<sup>[9]</sup> are given in the Supporting Information.
- [11] J.-F. Létard, *J. Mater. Chem.* **2006**, *16*, 2550–2559.
- [12] The  $\text{SbF}_6^-$  salt of this complex, **1**[ $\text{SbF}_6$ ]<sub>2</sub>, behaves differently again. It is not isostructural with **1**[ $\text{BF}_4$ ]<sub>2</sub> or **1**[ $\text{ClO}_4$ ]<sub>2</sub> and remains high-spin between 5–300 K. That was attributed to a strongly twisted ligand conformation in the crystal structure of **1**[ $\text{SbF}_6$ ]<sub>2</sub>, caused by a close intermolecular C–H... $\pi$  contact in the lattice.<sup>[14]</sup>
- [13] M. Hostettler, K. W. Törnroos, D. Chernyshov, B. Vangdal, H.-B. Bürgi, *Angew. Chem.* **2004**, *116*, 4689–4695; *Angew. Chem. Int. Ed.* **2004**, *33*, 4589–4594; R. Pritchard, S. A. Barrett, C. A. Kilner, M. A. Halcrow, *Dalton Trans.* **2008**, 3159–3168 and **2009**, 10621 (correction); B. Weber, W. Bauer, T. Pfaffeneder, M. M. Dîrtu, A. D. Naik, A. Rotaru, Y. Garcia, *Eur. J. Inorg. Chem.* **2011**, 3193–3206.
- [14] J. Elhaik, C. A. Kilner, M. A. Halcrow, *Dalton Trans.* **2006**, 823–830.
- [15] M. A. Halcrow, *Coord. Chem. Rev.* **2009**, *253*, 2493–2514.
- [16] P. Guionneau, M. Marchivie, G. Bravic, J.-F. Létard, D. Chasseau, *Top. Curr. Chem.* **2004**, *234*, 97–128.
- [17] R. Pritchard, C. A. Kilner, M. A. Halcrow, *Chem. Commun.* **2007**, 577–579.
- [18] A. Santoro, R. Kulmaczewski, L. J. Kershaw Cook, M. A. Halcrow, *Dalton Trans.*, in the press.
- [19] V. A. Money, J. Elhaik, I. R. Evans, M. A. Halcrow, J. A. K. Howard, *Dalton Trans.* **2004**, 65–69; R. Mohammed, G. Chastanet, F. Tuna, T. L. Malkin, S. A. Barrett, C. A. Kilner, J.-F. Létard, M. A. Halcrow, *Eur. J. Inorg. Chem.* **2013**, 819–831.
- [20] L. Pauling, *The Nature of the Chemical Bond*, 3<sup>rd</sup> edn., Cornell University Press, Ithaca NY, USA, **1960**, pp. 257–264.
- [21] R. Kulmaczewski, H. J. Shepherd, O. Cespedes, M. A. Halcrow, *Inorg. Chem.*, in the press.
- [22] C. J. O'Connor, *Prog. Inorg. Chem.* **1982**, *29*, 203–283.
- [23] G. M. Sheldrick, *Acta Cryst. Sect. A* **2008**, *64*, 112–122.
- [24] L. J. Barbour, *J. Supramol. Chem.* **2001**, *1*, 189–191.